Available online at www.sciencedirect.com
ScienceDirect
Engineering Structures 29 (2007) 1074–1083
ENGINEERING STRUCTURES
www.elsevier.com/locate/engstruct

Design of FRP confinement for square concrete columns

Shamim A. Sheikh[a,*], Yimin Li[b]

[a] *Department of Civil Engineering at the University of Toronto, Toronto, Ontario, Canada*
[b] *Hatch Acres Incorporated, Oakville, Ontario, Canada*

Received 4 August 2005; received in revised form 20 February 2006; accepted 18 July 2006
Available online 26 September 2006

Abstract

A procedure for the design of confining fibre-reinforced polymer (FRP) reinforcement in square concrete columns to enhance their seismic resistance is presented. In previous research, a method was developed for the design of confining steel in square reinforced concrete columns [Sheikh SA, Khoury SS. A performance-based approach for the design of confining steel in tied columns. ACI Struct J 1997;94(4):421–31]. Patterned on the same philosophy, the procedure presented here allows a designer to calculate the amount of confining FRP required for a certain ductility performance given the axial load on the column and the properties of the FRP. The required FRP content increases with an increase in ductility demand and an increase in the level of axial load applied. The procedure can be applied to new and existing square concrete columns and is corroborated with the experimental results obtained from realistically sized columns tested under simulated earthquake loads.

Keywords: Columns; Confinement; Ductility; Earthquake; Energy dissipation; Retrofitting

1. Introduction

Many of the existing reinforced concrete structures built according to pre-1970 design codes may not have sufficient ability to resist severe earthquakes. A major deficiency of these structures has been the inadequate amount of confinement reinforcement in potential plastic hinge regions of the columns that results in brittle structural response during earthquakes. To provide additional confinement to these deficient columns, retrofitting with fibre-reinforced polymer (FRP) jackets provides a very attractive solution due to their lightweight, high strength and excellent corrosion resisting capabilities. The current design code provisions [2,3] require large amounts of steel reinforcement placed at small spacing in critical regions of columns, which, quite often, makes construction very cumbersome and at times impractical. Use of external FRP shells with fibres aligned in the circumferential direction of the column can provide confinement and act as formwork for new structures.

Many experimental studies [4–12] have confirmed that the confinement provided by the FRP wraps can significantly increase the energy absorption capacity and ductility of the columns under combined axial, flexural and shear loads, thereby increasing their seismic resistance. This technique is gaining popularity in the field and a rational yet easy to use method is needed for the design of confining FRP so that practicing engineers can implement this new technology with confidence. It is generally agreed that circular confinement, due to its intrinsic nature, is considerably more efficient than square confinement. This paper is focused on square columns partly because of the availability of extensive data from well-instrumented square columns tested in a similar manner under simulated earthquake loads. Experimental and analytical work on circular columns is in progress on similar lines. Preliminary results indicate that the amount of FRP reinforcement required in circular columns is about half of what is required in square columns for similar improvement in ductility.

2. Proposed design approach

In order to develop a procedure for the design of confining FRP for square concrete columns, an extensive review of the available test results was conducted. Table 1 lists some of the available results from the tests on square or rectangular FRP-confined concrete columns under constant axial load and cyclic

* Corresponding author. Tel.: +1 416 978 3671; fax: +1 416 978 7046.
E-mail address: sheikh@ecf.utoronto.ca (S.A. Sheikh).

0141-0296/$ - see front matter
doi:10.1016/j.engstruct.2006.07.016

Table 1
Available tests on FRP-confined rectangular or square columns tested under cyclic lateral loads and constant axial loads

Researcher	No. of columns	Size and shape of specimens	Concrete strength (MPa)	Longitudinal steel		Lateral steel @ test region			FRP composite wraps @ test region			$\frac{P}{P_o}$
				f_y (MPa)	ρ_t (%)	f_y (MPa)	s (mm)	ρ_s (%)	Ultimate tensile strength	Thickness/Layer (mm)	Type and total layers	
Saadatmanesh et al. [7]	2	241 mm × 368 mm 1.892 m tall with one end stub	34.9 and 33.4	359	2.70[a] and 5.45	301	114.3	0.133	532 MPa	0.80	GFRP 8	0.16
Ma et al. [8]	1	410 mm square, 2.34 m tall with two end stubs	29	462	3[a]	455	300	0.45	606 MPa	1.0	CFRP 6	0.2
Iacobucci et al. [4]	7	305 mm square, 1.47 m tall with one end stub	36.5–42.3	465	2.58	457	300	0.61	962 N/mm/layer	1.0	CFRP 1–3	0.33 and 0.56
Memon and Sheikh [5]	7	305 mm square, 1.47 m tall with one end stub	42.5–44.2	465	2.58	457	300	0.61	563 N/mm/layer	1.25	GFRP 1–6	0.33 and 0.56
Ghosh and Sheikh [9]	3	305 mm square, 1.47 m tall with one end stub	26.8–27.2	465	2.58[a]	492	300	0.37 and 0.61	1019 N/mm/layer	1.0	CFRP 1	0.05 and 0.33
Javaid and Sheikh [10]	4	305 mm square, 1.47 m tall with one end stub	28.5	465	2.58[a]	509	300	0.37 and 0.61	563 N/mm/layer	1.25	GFRP 2 and 3	0.05 and 0.33
Ozbakkaloglu and Saatcioglu [11]	2	270 mm square, 1.72 m tall with one end stub	90	475 and 500	1.68 and 3.36	One column with 4 FRP crossties @ 68 mm spacing			3800 MPa	0.165	CFRP 5	0.32
Hosseini et al. [12]	2	260 mm square, 1.65 m tall with one end stub	53 and 52	420	1.5 and 3	420	120	1.36 and 1.8	3500 MPa	0.16	CFRP 3	0.15

[a] Longitudinal bars with lap splices in test regions.

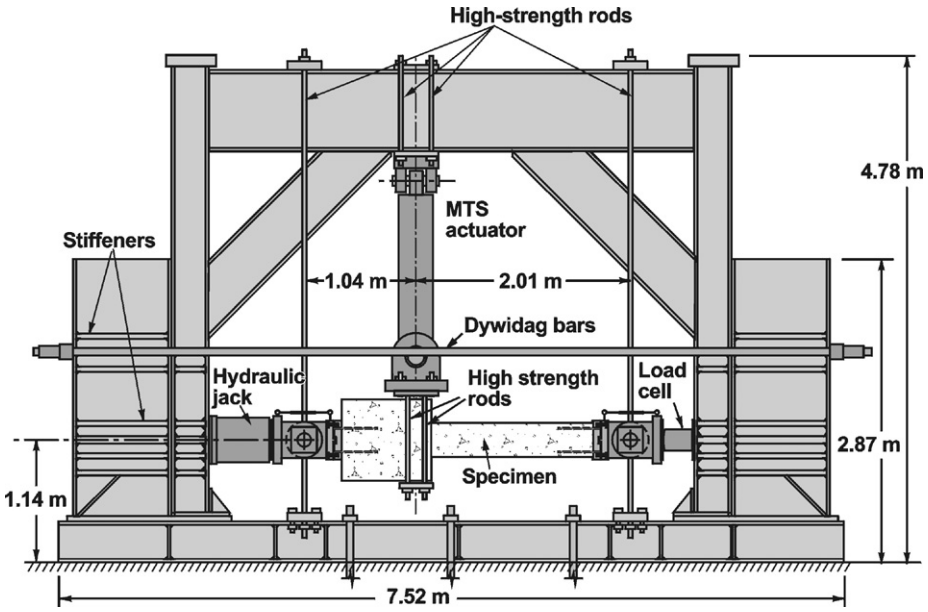

Fig. 1. Schematic test setup.

lateral load. This review indicated that the results available are limited. Although there exists a consensus that confining FRP can significantly enhance the seismic performance and ductility of square or rectangular concrete columns, the test setups, loading histories, instrumentations, specimen details and ductility parameters used in the available experimental investigations were different from one programme to another, making it difficult to evaluate these results on a common platform. Among these results, the columns tested by Iacobucci et al. [4] and Memon and Sheikh [5] were tested under similar conditions. More importantly, in these tests the specimens were similar and the moment–curvature behaviour of the most damaged regions of the specimens was reported, which is essential for the calculation of the ductility parameters used in the proposed design procedure. For these reasons, only these experimental results were used to corroborate the proposed design procedure. Also, since the procedure was developed for columns with continuous longitudinal rebar in plastic hinge regions, test data of columns with lap spliced longitudinal bars in plastic hinge regions were not considered when developing the procedure.

The proposed design approach was developed on the pattern of the procedure for the design of steel confining reinforcement [1]. The parameters used for evaluating the ductile performance of a column include section and member ductility, energy dissipation capacity and the number of standard displacement excursions a column could sustain before failure. Detailed development of this design procedure is available elsewhere [1,13]. However, some background data and the derivation of the procedure are briefly explained here.

2.1. Experimental results and ductility parameters

The proposed approach was developed using the experimental results of ten realistically sized FRP-confined specimens reported by Iacobucci et al. [4] and Memon and Sheikh [5]. In these experimental programmes, reinforced concrete columns with 305 mm square sections were tested under cyclic shear and flexure while simultaneously subjected to constant axial load to simulate earthquake loads, as shown in Fig. 1. The lateral displacement excursion regime consisted of one cycle to a displacement of $0.75\Delta_1$ followed by 2 cycles each of Δ_1, $2\Delta_1$, $3\Delta_1$ and so on until the specimen was unable to sustain the applied axial load. Analytical yield displacement Δ_1 was the lateral deflection corresponding to the estimated maximum lateral load along a load–deflection line that represented the initial stiffness of the column. Each specimen consisted of a 1.47 m long column cast integrally with a 510 × 760 × 810 mm stub that represented a beam–column joint or a footing. The columns were internally reinforced with steel and externally confined by different amounts of continuous CFRP or GFRP wraps. The ultimate tensile strength and rupture strain of the CFRP fabric were 962 N/mm width per layer and 0.0126, respectively, while these values for the GFRP fabric were 563 N/mm width per layer and 0.0228, respectively. In addition, three steel-confined columns without FRP wraps, i.e. AS-1NS, AS-8NS, and AS-1NSS, were tested as control specimens. Table 2 lists the details of the specimens considered in this study.

In evaluating the seismic performance of the columns and studying the effects of different variables, ductility and toughness parameters defined in Fig. 2 were used [1]. These include curvature ductility factor μ_ϕ, cumulative ductility ratio N_ϕ, and energy-damage indicator E. Subscripts t and 80 indicate, respectively, the value of the parameter until the end of the test (total value) and the value until the end of the cycle in which the moment has dropped to 80% of the maximum value. The energy parameter e_i represents the area enclosed in cycle i by the M–ϕ loop. Terms L_f and h represent the length of the most damaged region measured from the test and the depth of the column section, respectively. All other terms are defined in Fig. 2. The energy-damage indicator E is similar to the one proposed by Ehsani and Wight [14] for force–deflection curves.

Table 2
Member and section ductility parameters of FRP-confined columns

Researchers	Specimen	f'_c (MPa)	Lateral steel		Layers and type of FRP	Axial load level P/P_o	$\mu_{\phi 80}$	Ductility ratio		Energy indicator		$f_{l,\max}$ (MPa)	$\frac{f_{l,\max}}{f'_c}$
			Size @ Spacing (mm)	ρ_s (%)				$N_{\phi 80}$	$N_{\phi t}$	E_{80}	E_t		
Iacobucci et al. [4]	AS-1NS[a]	31.4	US#3@300	0.61	0	0.33	5.3	8	24	11	66	0	0
	ASC-2NS	36.5	US#3@300	0.61	1CFRP	0.33	11.6	61	73	352	466	6.3	0.17
	ASC-3NS	36.9	US#3@300	0.61	2CFRP	0.56	10.9[b]	56[b]	56	326[b]	326	12.6	0.34
	ASC-4NS	36.9	US#3@300	0.61	1CFRP	0.56	7.4[b]	24[b]	24	79[b]	79	6.3	0.17
	ASC-5NS	37.0	US#3@300	0.61	3CFRP	0.56	15.6[b]	109[b]	109	1083[b]	1083	18.9	0.51
	ASC-6NS	37.0	US#3@300	0.61	2CFRP	0.33	16.7[b]	161[b]	161	1328[b]	1328	12.6	0.34
	AS-8NS[a]	42.3	US#3@300	0.61	0	0.56	2.6[b]	5.4[b]	5.4	7.9[b]	7.9	0	0
Memon and Sheikh [5]	AS-1NSS[a]	42.4	US#3@300	0.61	0	0.56	2.6[b]	5.4[b]	5.4	7.9[b]	7.9	0	0
	ASG-2NSS	42.5	US#3@300	0.61	2GFRP	0.33	11.5	59	79	315	450	7.4	0.17
	ASG-3NSS	42.7	US#3@300	0.61	4GFRP	0.56	10.6[b]	55[b]	55	308[b]	308	14.8	0.35
	ASG-4NSS	43.3	US#3@300	0.61	2GFRP	0.56	7.1[b]	24[b]	24	97[b]	97	7.4	0.17
	ASG-5NSS	43.7	US#3@300	0.61	1GFRP	0.33	10.1	40	47	180	280	3.7	0.08
	ASG-6NSS	44.2	US#3@300	0.61	6GFRP	0.56	14.7[b]	135[b]	135	945[b]	945	22.2	0.50

[a] Control steel-confined specimens.
[b] Reduction in capacity less than 20% for completed cycles.

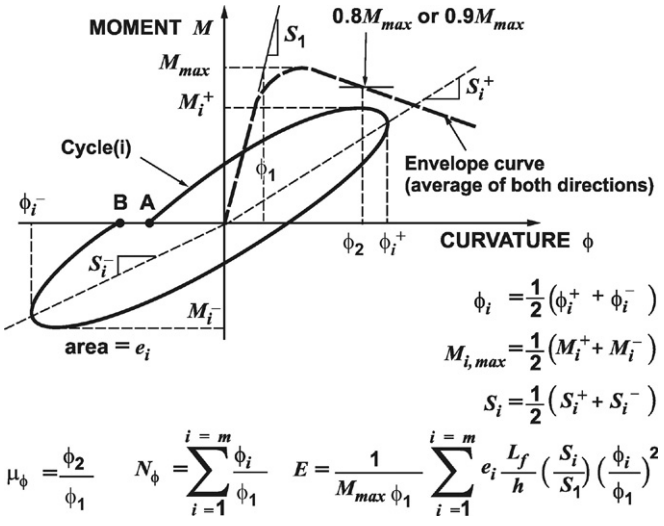

Fig. 2. Ductility parameters.

Table 2 lists these ductility and toughness parameters for the columns considered in this analysis.

2.2. Minimum requirements of ductility parameters

Sheikh and Khoury [1] have pointed out that different ductility and toughness parameters were interrelated. In columns internally confined with steel, for $\mu_{\phi 80}$ of 16, the values for $N_{\phi 80}$ and E_{80} were found to be 64 and 575, respectively. A column with this level of deformability was defined as highly ductile. The section with a $\mu_{\phi 80}$ value of 8 to 16 was defined as moderately ductile and the low ductility column had $\mu_{\phi 80} < 8$.

In order to compare the relationships between different ductility parameters of steel-confined columns with those of

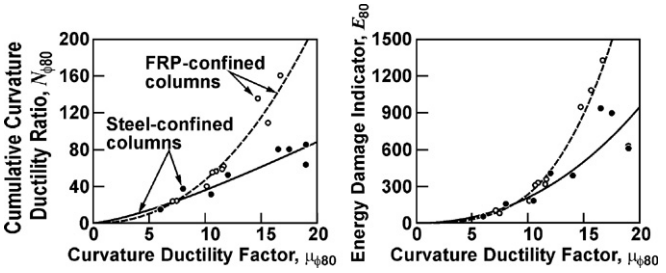

Fig. 3. Relationships between ductility parameters.

FRP-confined columns, curvature ductility factors, $\mu_{\phi 80}$, are plotted against cumulative curvature ductility ratios, $N_{\phi 80}$, and energy-damage indicators, E_{80}, in Fig. 3. Data from nine steel-confined column specimens reported by Sheikh and Khoury [1] and ten FRP-confined column specimens as listed in Table 2 are used to construct the figure.

From Fig. 3, it can be seen that up to $\mu_{\phi 80}$ of approximately 8, the curves for steel-confined and FRP-confined columns are very similar. For values of $\mu_{\phi 80}$ larger than 8, the values of $N_{\phi 80}$ and E_{80} of the FRP-confined columns are significantly higher than those of the steel-confined columns with similar $\mu_{\phi 80}$ values. It is obvious that for dissipating equal amounts of energy, the curvature ductility factors of the FRP-confined columns are smaller than those of the comparable steel-confined columns. This can be attributed to the different curvature distributions in the plastic hinge region and different plastic hinge lengths in these two types of columns. For similar steel-confined columns tested in the same manner, the equivalent plastic hinge length was reported to be approximately equal to the dimension of the cross section [15,16], whereas the equivalent plastic hinge length of most of the FRP-confined columns was observed to be larger than the section dimension [4,5].

For steel-confined columns, a $\mu_{\phi 80}$ value of 16 corresponds to $E_{80} = 575$, while a $\mu_{\phi 80}$ value of 8 corresponds to $E_{80} = 123$. From the curves for FRP-confined columns in Fig. 3, it can be seen that at $E_{80} = 575$, the corresponding value for $\mu_{\phi 80}$ is 13.2; while at $E_{80} = 123$, the corresponding value for $\mu_{\phi 80}$ is 8.2. Considering the energy dissipation capacity, the behaviour of a FRP-confined column with $\mu_{\phi 80} = 13$ can be considered as highly ductile. The section with a $\mu_{\phi 80}$ value of 8 to 13 can thus be defined as moderately ductile and the low ductility column has $\mu_{\phi 80} < 8$.

2.3. Design procedure

Sheikh and Khoury [1] proposed a procedure for the design of confining steel for square steel-confined columns. The design equations were as follows:

$$A_{sh} = \alpha \cdot 0.3 s h_c \left(\frac{A_g}{A_{ch}} - 1\right) \frac{f'_c}{f_y} \cdot Y_P \cdot Y_\phi \geq \alpha \cdot 0.09 s h_c \frac{f'_c}{f_y} \cdot Y_P \cdot Y_\phi \quad (1)$$

where A_{sh} is the total cross sectional area of rectilinear steel perpendicular to dimension h_c; α is confinement efficiency parameter related to steel configuration; s is tie spacing; h_c is the dimension of concrete core measured to the outside of perimeter tie; A_g is gross area of section; A_{ch} is area of the concrete core measured to the outside of perimeter tie; f'_c is compressive strength of concrete; f_y is yield strength of lateral steel; Y_P is a parameter to take into account the effect of axial load and taken as:

$$Y_P = 1 + 13 \cdot \left(\frac{P}{P_o}\right)^5 \quad (2)$$

and Y_ϕ is a parameter to take into account the section ductility demand and taken as:

$$Y_\phi = \frac{\mu_{\phi 80}^{1.15}}{29.0}. \quad (3)$$

Sheikh and Khoury [1] also suggested the following simplified linear expressions for Y_P and Y_ϕ:

$$Y_P = 6\frac{P}{P_o} - 1.4 \geq 1 \quad (4)$$

$$Y_\phi = \frac{\mu_{\phi 80}}{18}. \quad (5)$$

Eq. (1) can be rearranged as

$$\frac{f_l}{f'_c} = \alpha \cdot 0.3 \left(\frac{A_g}{A_{ch}} - 1\right) \cdot Y_P \cdot Y_\phi \geq \alpha \cdot 0.09 \cdot Y_P \cdot Y_\phi \quad (6)$$

where f_l is the lateral confining pressure exerted by the lateral steel to the concrete core and can be calculated as

$$f_l = \frac{A_{sh} \cdot f_y}{s \cdot h_c}. \quad (7)$$

From Eq. (6), it can be observed that the required lateral confining pressure normalized with respect to the concrete strength f'_c, which can be defined as the confinement ratio [17], increases with an increase in axial load level or an increase in ductility demand. The required confinement ratio also depends on the confinement efficiency of the lateral reinforcement. The higher the confinement efficiency of the lateral steel, the lower the required confinement ratio. The design method when applied to realistically sized specimens tested by different investigators yielded excellent agreement with the experimental results.

2.4. Design considerations for square FRP-confined columns

Based on the experimental results listed in Table 2, the most important variables identified to affect a column's ductility are the amount of FRP confining reinforcement, type of FRP and the level of axial load. The effect of these variables on column behaviour is discussed in the following.

2.4.1. Amount of confining FRP

The effect of the amount of confining CFRP can be evaluated by comparing the moment vs. curvature behaviour of two sets of columns, as presented in Fig. 4. The first set includes Specimens AS-1NS, ASC-2NS and ASC-6NS that were tested under an axial load of $0.33P_o$. All the columns in the second set, AS-1NSS, ASC-4NS, ASC-3NS, and ASC-5NS, were tested under an axial load of $0.56P_o$. The ductility parameters in Table 2 and the responses shown in Fig. 4 clearly demonstrate the enhanced cyclic performance of the FRP-retrofitted columns. The behaviour of columns improved progressively as the amount of confining CFRP increased. While Specimen AS-1NS tested under axial load of $0.33P_o$ failed following the 7th cycle, Specimen ASC-2NS, which was confined by one layer of CFRP, failed during the 15th load cycle and Specimen ASC-6NS, confined with two layers of CFRP, was able to sustain 20 load cycles. The ductility parameters of Specimens ASC-2NS and ASC-6NS are also significantly larger than those of Specimen AS-1NS. The columns tested under higher axial load, ASC-4NS, ASC-3NS, and ASC-5NS, were able to sustain 8, 11, and 15 load cycles, respectively while the control specimen AS-1NSS failed in the fourth cycle. The enhancements in curvature ductility of the columns were approximately proportional to the amount of confining FRP provided. Comparisons of the behaviour of the GFRP-confined columns and the control specimens as shown in Fig. 5 and Table 2 also lead to the same conclusion. It should be noted that minimal lateral steel reinforcement was used in all the columns with spacing equal to the size of the column section. The confinement effectiveness of such reinforcement is known to be insignificant and is obvious from the behaviour of columns AS-1NS, AS-8NS, and AS-1NSS.

2.4.2. Axial load level

Another important variable that determines the behaviour of a column particularly with respect to ductility is the level of axial load applied. The effect of this parameter can be evaluated by comparing the behaviour of Specimens ASC-2NS and ASC-4NS, which were almost identical in every respect except for

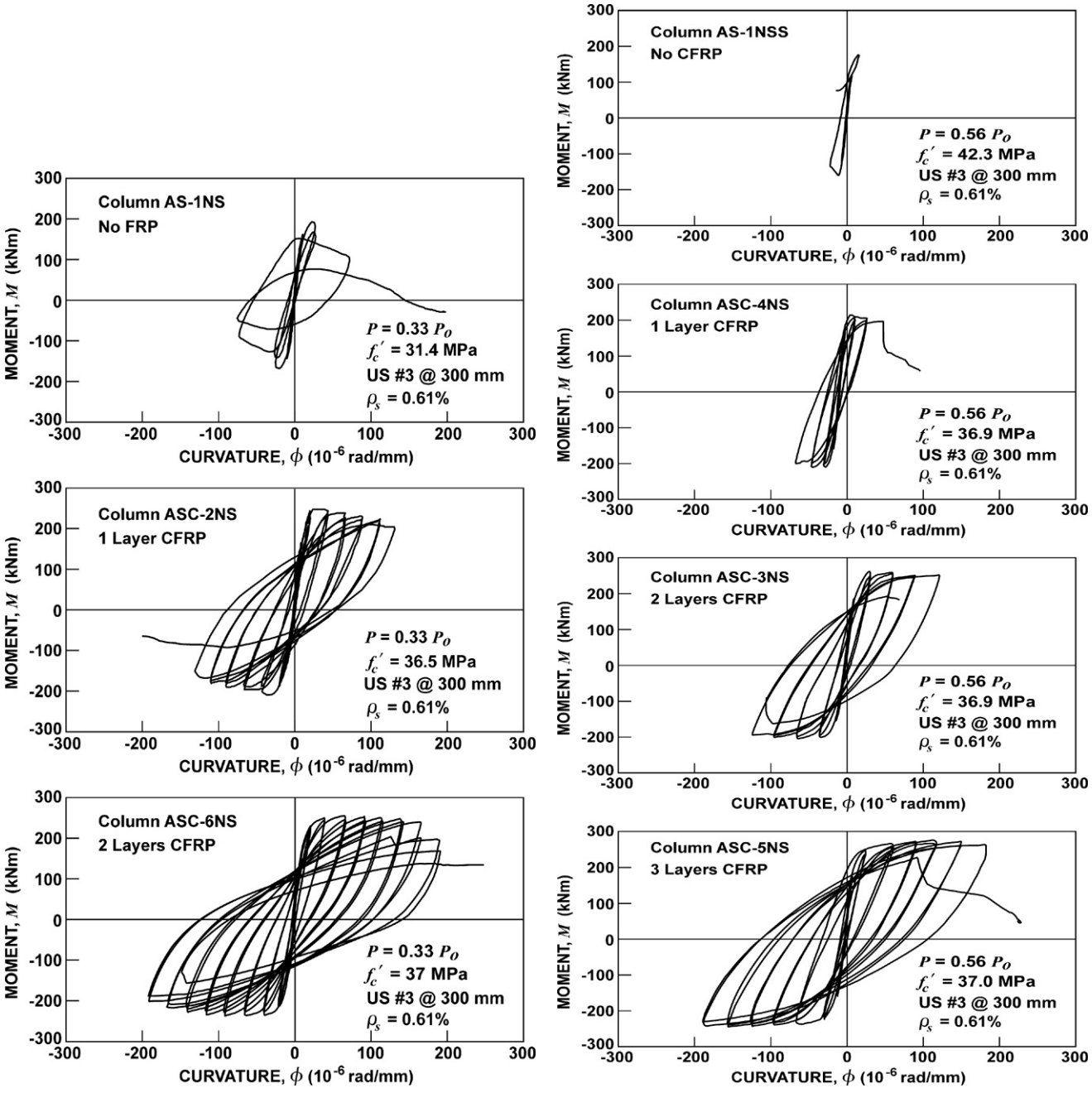

(a) Specimens tested under an axial load of $0.33P_o$.

(b) Specimens tested under an axial load of $0.56P_o$.

Fig. 4. Behaviour of CFRP-confined specimens.

the different levels of axial load applied. An increase in axial load from $0.33P_o$ in ASC-2NS to $0.56P_o$ in ASC-4NS resulted in significantly less ductile behaviour. The column resisting a high axial load experienced a decline in ductility ratio of approximately 60% and dissipated energy of about 75%. Its excursion limit was also reduced to 8 cycles from 15 for the specimen under lower axial load. Similar observations can be made by comparing the behaviour of Specimens ASC-6NS and ASC-3NS in Fig. 4. Specimens ASG-2NSS and ASG-4NSS confined with two layers of GFRP can also be compared to evaluate the effect of axial load (Fig. 5). Increase in axial load from $0.33P_o$ to $0.56P_o$ reduced the ductility factor from 11.5 to 7.1. The energy dissipation for ASG-2NSS tested under lower axial load is approximately 4.7 times larger than the energy dissipated by specimen ASG-4NSS. Inclusion of specimen ASG-3NSS in the comparison shows that the effects of the higher axial load can be countered by an increase in the lateral FRP confinement. Specimen ASG-3NSS was strengthened with 4 layers of GFRP and tested at high axial load of $0.56P_o$. Moment–curvature responses of ASG-2NSS and ASG-3NSS are very similar with ASG-2NSS displaying a little more ductile behaviour.

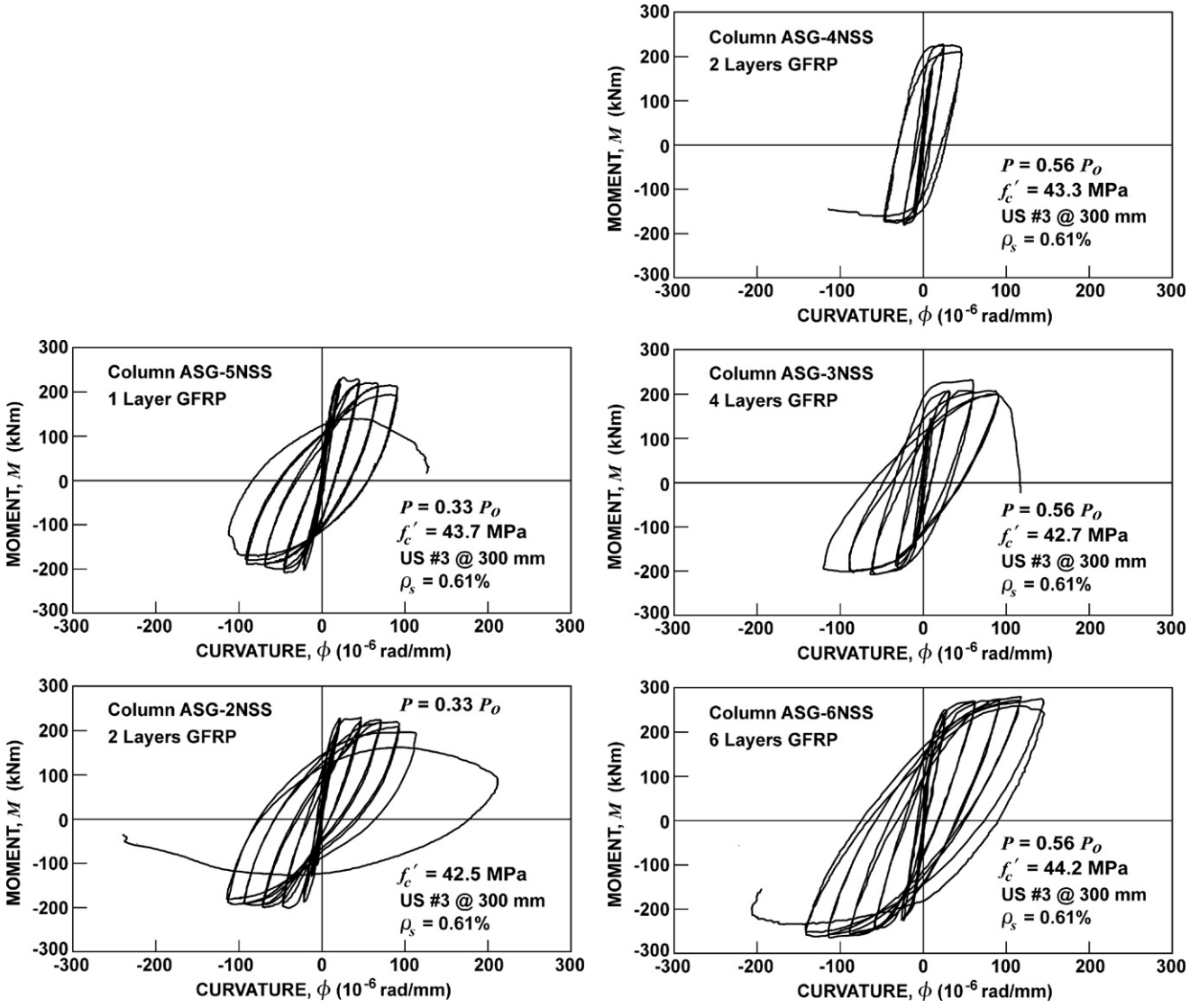

(a) Specimens tested under an axial load of $0.33P_o$.

(b) Specimens tested under an axial load of $0.56P_o$.

Fig. 5. Behaviour of GFRP-confined specimens.

2.4.3. Type of confining FRP

The relative effectiveness of CFRP and GFRP in strengthening deficient columns can be evaluated by comparing the behaviour of four sets of specimens: ASC-2NS and ASG-2NSS, ASC-3NS and ASG-3NSS, ASC-4NS and ASG-4NSS, and ASC-5NS and ASG-6NSS. The two columns in each set of specimens are similar in every aspect except that one column was confined by CFRP whereas the other one was confined by GFRP. The layers of the GFRP were twice as many as those of the CFRP. Comparisons of the ductility parameters given in Table 2 and the moment–curvature relationships in Figs. 4 and 5 show that both columns in each set behaved in a similar manner and had comparable ductility parameters, indicating that the confinement effectiveness of two layers of GFRP is similar to that of one layer of CFRP. It is worth noting that in these tests, the ultimate tensile strength of the CFRP fabric was approximately 70% higher than that of the GFRP fabric. The stiffness of CFRP measured in terms of N/mm width per layer was about three times larger than that of GFRP. From these test results, it appears that the effectiveness of FRP in enhancing column ductility closely relates to its ultimate tensile strength.

2.4.4. Design equations

From the above discussion, it can be concluded that for square FRP-confined columns, the column ductility increases as the amount of confining reinforcement increases, whereas an increase in axial load level reduces column ductility. These effects are similar to those in steel-confined columns reported by Sheikh and Khoury [1]. In spite of these similarities between steel-confined and FRP-confined columns, there are also some major differences between these two types of columns that must be taken into account in design considerations. Firstly, in reinforced concrete columns, the lateral steel is used internally to confine the concrete. The core concrete within the lateral steel is confined whereas the cover concrete outside the lateral steel is not. Hence as the thickness of the cover concrete

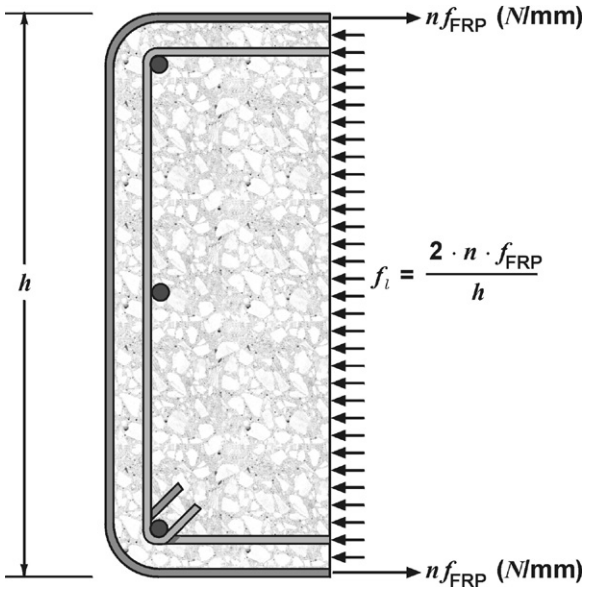

Fig. 6. Lateral confining pressure provided by FRP in square columns.

increases, the area of the confined concrete decreases. As a result, more confinement reinforcement will be required to achieve a certain ductility performance. The A_g/A_{ch} ratio in Eq. (1) for steel-confined columns takes into account this effect. In FRP-confined columns, however, the FRP wraps are used externally thus confining the entire cross section of the column. Therefore, the thickness of the cover concrete has no effect on column behaviour and need not be considered as a design parameter. Another important difference is the nature of the lateral confining pressure exerted by steel and FRP. In steel-confined columns undergoing inelastic deformations, the confining pressure remains practically constant while the steel yields under hoop tension. In columns continuously confined by FRP, on the other hand, the lateral confining pressure is not constant. As the concrete core expands laterally and the lateral strain increases, the confining pressure keeps increasing up to the rupture of fibres due to the linear elastic stress–strain characteristic of the FRP.

For square columns confined by FRP as shown in Fig. 6, the lateral confining pressure provided by the FRP, f_l, can be calculated as:

$$f_l = \frac{2 \cdot n \cdot f_{FRP}}{h} \tag{8}$$

where n = number of layers of FRP; f_{FRP} = tensile stress in FRP and h = cross sectional dimension of column.

It is not always possible to measure the actual average strains of the FRP at the location of failure in a column. Strains measured elsewhere in FRP would generally be lower, which may lead to an incorrect assumption that FRP fails at a lower strain in a column than in a coupon test. Jaffry and Sheikh [18] have observed that tensile strains in FRP at failure of the columns under concentric compression were close to the rupture strain of FRP under axial tension. Iacobucci et al. [4] have also made similar observations for columns tested under combined loads. From the experimental results listed in Table 2,

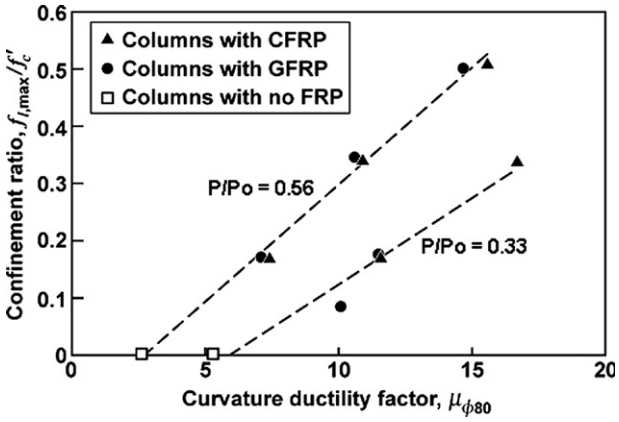

Fig. 7. Relationship between curvature ductility factor, $\mu_{\phi 80}$ and theoretical maximum lateral confining pressure provided by FRP, $f_{l,\max}$.

it was also found that there is a clear relationship between the curvature ductility factors of the columns and the theoretical maximum lateral confining pressure, $f_{l,\max}$, provided by the FRP, which can be defined as:

$$f_{l,\max} = \frac{2 \cdot n \cdot f_u}{h} \tag{9}$$

where f_u is the ultimate tensile strength of the FRP obtained from tensile coupon tests. Other terms are as defined earlier.

The theoretical maximum lateral confining pressures provided by FRP, $f_{l,\max}$, were calculated for the ten specimens and are listed in Table 2. The relationship between the curvature ductility factor and theoretical maximum lateral confining pressure provided by the FRP is shown in Fig. 7. In this figure, the theoretical maximum lateral confining pressures are normalized with respect to the unconfined concrete compressive strength of the columns, which can be defined as the confinement ratio for the columns [17].

Fig. 7 indicates that for a certain level of axial load, the curvature ductility factor, $\mu_{\phi 80}$, of a column increases almost linearly with the increase in the confinement ratio, as shown by the two dashed lines in the figure. This relationship can be expressed by the following equation:

$$\frac{f_{l,\max}}{f'_c} = \lambda \cdot Y_p \cdot Y_\phi \tag{10}$$

where λ is a constant and Y_P and Y_ϕ are parameters to take into account the effect of axial load and the section ductility demand. Substituting Eq. (9) into Eq. (10) and rearranging gives:

$$n \cdot f_u = \beta \cdot f'_c \cdot h \cdot Y_P \cdot Y_\phi \tag{11}$$

where β is a confinement efficiency parameter and equal to $\lambda/2$.

In the application of Eq. (11), along with Eqs. (2) and (3) suggested by Sheikh and Khoury [1], to the aforementioned FRP-confined columns, it was found that the expressions for Y_P and Y_ϕ for steel-confined concrete columns were equally applicable to FRP-confined columns. Substituting the expressions for Y_P and Y_ϕ (Eqs. (2) and (3)) into Eq. (11) gives

Table 3
Value of β

Specimen	$\mu_{\phi 80}$	Control specimen	$\mu_{\phi 80}$ of control specimen	$\mu_{\phi 80,\text{in}}$	Value of β
ASC-2NS	11.6	AS-1NS	5.3	6.3	0.29
ASC-3NS	10.9	AS-8NS	2.6	8.3	0.25
ASC-4NS	7.4	AS-8NS	2.6	4.8	0.24
ASC-5NS	15.6	AS-8NS	2.6	13.0	0.23
ASC-6NS	16.7	AS-1NS	5.3	11.4	0.29
ASG-2NSS	11.5	AS-1NS	5.3	6.2	0.29
ASG-3NSS	10.6	AS-1NSS	2.6	8.0	0.27
ASG-4NSS	7.1	AS-1NSS	2.6	4.5	0.26
ASG-5NSS	10.1	AS-1NS	5.3	4.8	0.19
ASG-6NSS	14.7	AS-1NSS	2.6	12.1	0.24
Average					0.25
Standard deviation					0.03

the following form of the design equation:

$$n \cdot f_u = \beta \cdot h \cdot f'_c \cdot \left\{1 + 13\left(\frac{P}{P_o}\right)^5\right\} \frac{\mu_{\phi 80,\text{in}}^{1.15}}{29} \tag{12}$$

where $\mu_{\phi 80,\text{in}}$ is the increase in curvature ductility factor due to FRP confinement and

$$\mu_{\phi 80,\text{in}} = \mu_{\phi 80} - \mu_{\phi 80,\text{con}} \tag{13}$$

where:
$\mu_{\phi 80}$ = curvature ductility factor of the FRP-confined specimen; and
$\mu_{\phi 80,\text{con}}$ = curvature ductility factor of the control reinforced specimen.
The experimental results of the ten FRP-confined columns were used to calculate the value for β using Eq. (12). The results are listed in Table 3. The average value of β is about 0.25 and the standard deviation is 0.03.

The simplified version of the above equation can be written as

$$n \cdot f_u = \beta \cdot h \cdot f'_c \cdot \left(6\frac{P}{P_o} - 1.4\right) \frac{\mu_{\phi 80,\text{in}}}{18} \geq \beta \cdot h \cdot f'_c \cdot \frac{\mu_{\phi 80,\text{in}}}{18}. \tag{14}$$

The experimental curvature ductility factors and analytical values obtained from Eqs. (12) and (14) are compared in Fig. 8. The average of the analytical curvature ductility factors using Eq. (12) is roughly equal to the average of the experimental values and the standard deviation from the mean is about 6%, whereas Eq. (14) is more conservative and slightly underestimates the curvature ductility of the columns in most cases.

The above design procedure is applicable to square normal strength concrete columns confined by continuous FRP wraps with continuous longitudinal rebar in plastic hinge regions. Its applicability to high strength concrete columns and columns confined by non-continuous FRP bands needs further investigation. The design procedure was corroborated with the test results on columns with 305 mm square sections, its applicability to columns with significantly different sizes is not confirmed due to a lack of such data.

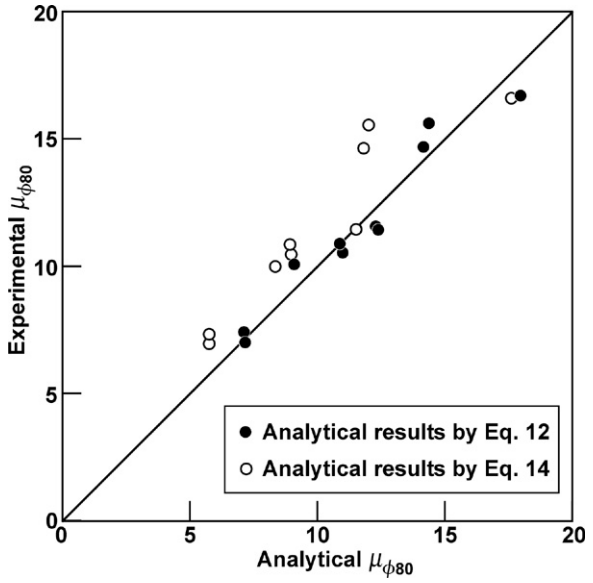

Fig. 8. Comparison of experimental and analytical curvature ductility factors.

3. Application of the proposed design approach

The proposed method is applied to a 450 mm square column reinforced with eight longitudinal bars of 25 mm diameter. The concrete compressive strength and FRP rupture strength are assumed to be 35 MPa and 900 N/mm width per layer, respectively. Yield strength of steel is taken as 400 MPa. Fig. 9 shows the number of layers needed as a function of the column axial load for two values of ductility enhancement. If it is assumed that the original steel-reinforced column is capable of displaying a ductility factor of 4, enhancements of $\mu_{\phi 80}$ by 4 and 9 would make the column moderately and highly ductile, respectively. Addition of one layer of FRP would make the column moderately ductile if the axial load is $0.5P/P_o$. For the same level of axial load, 2.4 layers of FRP are needed to make the column highly ductile thus requiring three layers of FRP wrap in practice. If three layers are used, the FRP strength can be as low as 720 N/mm width per layer. As stated earlier, about half the number of layers would be required for circular columns for similar ductility enhancements. It should be noted from Fig. 9 that the simplified equation is significantly

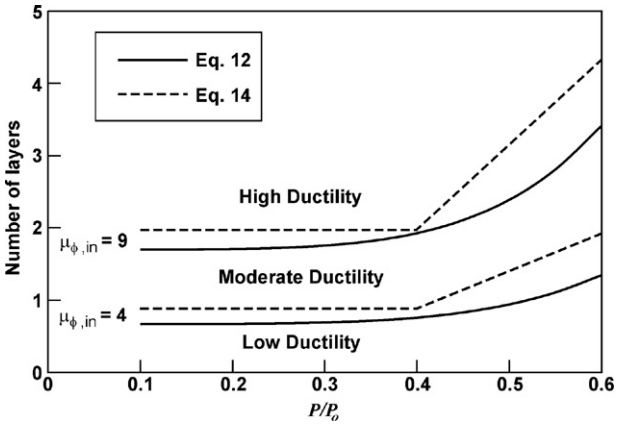

Fig. 9. Application of the design procedure.

conservative compared to the original equation particularly for high axial load levels.

4. Concluding remarks

A performance-based approach is presented for the design of confining FRP reinforcement externally applied to square concrete columns. The procedure is patterned on the design philosophy proposed by Sheikh and Khoury [1] for steel-confined columns and is corroborated with the experimental results of FRP-confined columns. Performance of a column is evaluated in terms of its ductility and energy dissipation capacity. The experimental results show that important variables that affect the ductility parameters of a square column include the level of axial load and the amount of confining reinforcement. The proposed procedure relates the confinement design parameters such as the amount of FRP reinforcement and FRP strength to the column's ductile performance. The required amount of confining FRP increases with an increase in ductility demand, an increase in the level of axial load applied and reduced FRP strength. An example demonstrating the application of the proposed procedure is also included.

Acknowledgments

The authors wish to express their gratitude and sincere appreciation to Natural Sciences and Engineering Research Council (NSERC) of Canada and ISIS Canada, an NSERC Network of Centre of Excellence for financing this research work.

References

[1] Sheikh SA, Khoury SS. A performance-based approach for the design of confining steel in tied columns. ACI Struct J 1997;94(4):421–31.
[2] CSA-A23.3-94. Design of concrete structures. Rexdale (Ontario, Canada): Canadian Standards Association; 1994.
[3] ACI Committee 318. Building code requirements for structural concrete (ACI 318-05). Farmington Hills (MI): American Concrete Institute; 2005.
[4] Iacobucci R, Sheikh SA, Bayrak O. Retrofit of square columns with carbon fibre reinforced polymers for seismic resistance. ACI Struct J 2003;100(6):785–94.
[5] Memon MS, Sheikh SA. Seismic behaviour of square concrete columns retrofitted with glass fibre-reinforced polymers. Research report. Ontario (Canada): Dept of Civ Eng, Univ of Toronto; 2002.
[6] Sheikh SA, Yau G. Seismic behaviour of concrete columns confined with steel and fibre-reinforced polymers. ACI Struct J 2002;99(1):72–80.
[7] Saadatmanesh H, Ehsani MR, Jin L. Repair of earthquake-damaged RC columns with FRP wraps. ACI Struct J 1997;94(2):206–15.
[8] Ma R, Xiao Y, Li KN. Full-scale testing of a parking structure column retrofitted with carbon fibre reinforced composites. J Construct Building Mater 2000;14(2):63–71.
[9] Ghosh KK, Sheikh SA. Seismic upgrade with CFRP of RC columns containing lap spliced rebars in plastic hinge regions. Research report. Ontario (Canada): Dept of Civ Eng, Univ of Toronto; 2002.
[10] Javaid U, Sheikh SA. Seismic upgrade with GFRP of RC columns containing lap spliced rebars in plastic hinge regions. Research report. Ontario (Canada): Dept of Civ Eng, Univ of Toronto; 2003.
[11] Ozbakkaloglu T, Saatcioglu M. Seismic performance of high-strength concrete columns cast in stay-in-place FRP formwork. In: Proceedings of 13th world conference on earthquake engineering. 2004.
[12] Hosseini A, Khaloo AR, Fadaee S. Seismic performance of high-strength concrete square columns confined with carbon fibre reinforced polymers (CFRP). Can J Civ Eng 2005;32(3):569–78.
[13] Li Y, Sheikh SA. Design of retrofitting FRP for concrete columns. Research report. Ontario (Canada): Dept of Civ Eng, Univ of Toronto; 2003.
[14] Ehsani MR, Wight JK. Confinement steel requirement for connection in ductile frames. J Struct Div, ASCE 1990;116(3):751–67.
[15] Sheikh SA, Khoury SS. Confined concrete columns with stubs. ACI Struct J 1993;90(4):414–31.
[16] Sheikh SA, Shah DV, Khoury SS. Confinement of high-strength concrete columns. ACI Struct J 1994;91(1):100–11.
[17] Samaan M, Mirmiran A, Shahawy M. Model of concrete confined by fibre composites. J Struct Eng, ASCE 1999;124(9):1025–31.
[18] Jaffry SAD, Sheikh SA. Concrete filled glass fibre reinforced ploymer (GFRP) shells under concentric compression, Research report: SJ-01-01. Ontario (Canada): Dept of Civ Eng, Univ of Toronto; 2001.